Molecular adsorption, self-assembly, and friction in lubricants

Molecular adsorption, self-assembly, and friction in lubricants

Rui F. G. Apóstolo, Georgia Tsagkaropoulou, and Philip J. Camp[1]

School of Chemistry, University of Edinburgh, David Brewster Road, Edinburgh EH9 3FJ, Scotland

Abstract

Lubricants are complex fluids consisting of a base oil and many different additives, and are used to control friction and wear between solid inorganic surfaces in relative motion. A review of recent work on molecular simulations of lubricants is given. It is shown that simulations can be used to uncover a lot of interesting behaviour, including additive adsorption, additive self-assembly, and a competition between the two. The specific examples to be discussed are: the adsorption of stearic acid and oleic acid in squalane on iron-oxide surfaces; the self-assembly of glycerol monooleate in bulk n-heptane; the adsorption and friction of glycerol monooleate in squalane on iron-oxide surfaces; and the conformations of functionalised copolymers in bulk n-heptane. The structures adopted by the additives can be correlated with the observed frictional properties, opening up the possibility of molecular-level design of new lubricants.

Keywords: adsorption; self-assembly; friction; lubricants; molecular dynamics simulations

1. Introduction

Engine lubricants are complex solutions of additives in a base-oil solvent. The base oil is a polydisperse mixture of aliphatic and aromatic hydrocarbons, and constitutes approximately 80 wt% of the lubricant. The remaining components include viscosity modifiers (typically polymers), dispersants (to keep

[1]Corresponding author. E-mail address: philip.camp@ed.ac.uk (P. J. Camp)

soot in the oil rather than being deposited on engine components), detergents (inorganic compounds that react with sludge precursors and neutralise acids), organic friction modifiers (OFMs), inorganic friction modifiers, and corrosion inhibitors. (Note that the use of the term 'detergent' here is different from the conventional definition of a water-soluble surfactant.) The complete formulation lubricates moving parts in the engine, which can be assumed to be metal or metal-oxide surfaces. Although passenger cars will crossover from internal combustion engines (ICEs) to electric power trains within the next few decades, there is still an urgent need to mitigate the effects of fuel consumption, CO_2 production, and engine-component wear during the transition period. Moreover, there is a move towards lower-viscosity base oils to improve fuel economy, and this places additional burdens on additives to reduce friction and wear within the engine. Friction accounts for approximately 10% of energy losses from the engine, and even a modest decrease in the frictional losses $\sim 1\%$ would translate to substantial reductions in emissions and CO_2, and financial savings to vehicle owners. An equally important market for fuels and lubricants is in marine shipping, which will rely on ICEs for the foreseeable future. A lot of work remains to be done to improve the longevity of marine engines, and hence reduce costs associated with servicing and replacement, and to mitigate the pollution arising from them [1].

This contribution focuses on the physical chemistry of OFMs, which encompasses a broad range of structural and dynamic phenomena at the solid-oil interface. OFMs are often surfactant-like molecules which are assumed to adsorb at interfaces, and provide soft layers which reduce friction between two solid surfaces brought together under load and sheared relative to one another. Some of the basic physical parameters are the (transient) loads on engine components (up to 10^9 Pa), the surface roughness and average surface separation (L) of engine components ($\sim \mu$m), and the relative sliding velocity ($v_\mathrm{s} = 0.1$–10 m s^{-1}). These parameters give corresponding shear rates of $\dot{\gamma} = v_\mathrm{s}/L = 10^5$–$10^7$ s^{-1}.

Typical OFMs can form surface layers of around 2 nm thickness, so how do they control friction? The answer is that the load is supported at asperity

contacts, where the peaks on one solid surface are in very close contact with the peaks on the other surface. At these contacts, the local separation is smaller, and the shear rate is higher, than the engineering parameters given above, but these are the conditions under which the OFMs operate. To put this in context, the relationship between the OFM layer and the surface roughness is similar to that between a blade of tall grass (1 m) and the height of a mountain (1000 m).

The classical picture of lubrication is that the OFMs adsorb on a surface to form a monolayer [2, 3, 4] driven by the attraction of the polar head groups with the inorganic surface, and the favorable interactions between the non-polar tails and the base oil. This is shown schematically in Fig. 1(a). This is thought to increase the degree of slip between two surfaces, the adsorbed layers, and any confined liquid. Experimental investigations of strongly confined liquids under extremes of pressure and shear are difficult to carry out. Although the structures and adsorbed films can be investigated under quiescent conditions using techniques such as X-ray or neutron reflectometry, and sum frequency generation (SFG) spectroscopy, carrying out these experiments *in situ* is extremely challenging. Molecular simulations provide valuable insights into the structure and dynamics on length scales appropriate to the asperity contact (0.1–10 nm), and can be used to correlate molecular structure with tribological properties. Equilibrium and non-equilibrium molecular dynamics (MD) simulations have been used extensively to examine the structure, dynamics, and tribological properties of lubricants [5, 6]. Examples include pure polymer melts and hydrocarbons [7, 8, 9, 10, 11, 12, 13, 14], silanes [15], fatty acids and amines [16, 17, 18, 19, 20, 21], glycerin [22], glycerides [23], zinc dialkyldithiophosphates [24], MoS_2 [25, 26], room-temperature ionic liquids [27, 28], and carbon nanoparticles [29].

For both experiment and simulation, one of the major problems is the sheer complexity of lubricants, and the evolving chemical and physical characteristics of the surfaces. In both types of research, simple model systems are required to start building up an understanding of how lubricants work. To this end, the main message of this contribution is that, on the basis of molecular simulations,

there are well-known OFMs that do not form simple monolayer structures, and that self-assembly in bulk and at interfaces can compete with surface adsorption and have substantial effects on the resulting friction. Some competing structures are shown in Fig. 1(b). A hemi-micelle can be adsorbed on the surface, whereby the polar head groups are attracted to each other and the inorganic surface, and the non-polar tail groups are solvated by the base oil. Alternatively, the surfactant can remain in the liquid layer as a complete reverse micelle, with the polar head groups forming a core, and the non-polar tail groups immersed in the base oil. Any water in the system will prefer to be at the inorganic surfaces and/or in the cores of reverse micelles [30, 31].

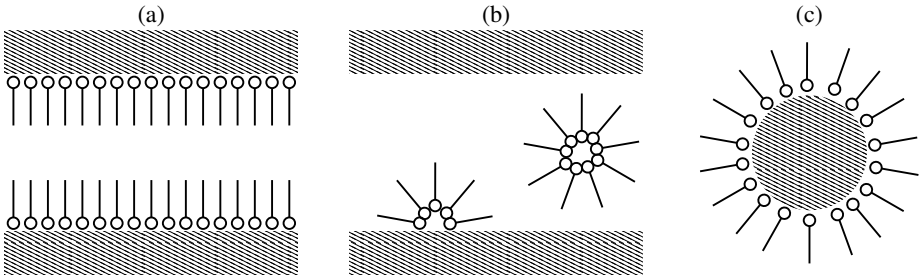

Figure 1: Schematic diagrams of (a) monolayer adsorption at planar interfaces, (b) adsorption and self-assembly between planar interfaces, and (c) monolayer adsorption at a curved interface. Surfactant molecules are shown as polar head groups (circles) with non-polar tails. Solid surfaces are shown as hatched areas.

In this article, a short review of recent molecular-simulation work on the properties of OFMs is given. The rest of the article is arranged as follows. A brief overview of the relevant MD simulation methods is given in Sec. 2. In Sec. 3, the conventional case of monolayer adsorption is discussed with respect to the effects of surface curvature, and the dependence of the adsorbed-film properties on molecular details. Section 4 is dedicated to the occurrence of self-assembly in bulk non-aqueous liquids. The competition between adsorption and self-assembly in confined liquids is illustrated in Sec. 5, along with the effects on friction.

2. Simulation methods

Standard equilibrium MD simulations in the NVT and NPT ensembles can be applied to the study of adsorption and self-assembly in both bulk and confined-liquid systems [32, 33]. Simulations are carried out with periodic boundary conditions applied, either in all three directions (bulk systems) or in two directions (systems in a slit pore). Temperature and pressure are controlled with a standard method, such as the Nosé-Hoover thermostat/barostat. Typically, self-assembly of surfactant-type additives can be observed on the ten-nanosecond time scale, while sampling the full range of conformations of polymeric additives may require simulations of several hundred nanoseconds (see Sec. 4).

The full range of non-equilibrium molecular-simulation methods for studying lubrication phenomena has been reviewed recently [6]. For the study of liquid properties under confinement and shear, a thermostat is required to remove the excess heat energy arising from work being done on the system against viscous and friction forces. There are several methods for doing this, but in the work reviewed here, temperature is controlled by thermostatting the system only in the y direction, while the system is sheared in the xz plane. This ensures that the velocity profile $v_x(z)$ is not strongly influenced by the thermostat, at least for the liquid layers described here, which are typically around 10 nm thick. For thin liquid layers – on the order of several molecular diameters – the observed properties can depend sensitively on the method of temperature control [34, 35]. Of particular importance is the conduction of heat from the liquid layer in to the solid surfaces, and hence rigid walls are not appropriate for such simulations. The load on a confined liquid can be controlled directly by applying forces to the outermost layers of atoms in the solid surfaces, without having to apply an extended-Hamiltonian barostat. Non-equilibrium MD simulations can routinely be carried out on the 10–100 ns time scale. Steady-state velocity profiles in the liquid layer are established quite quickly ($\sim$ 10 ns), but long runs may be necessary to gather sufficient statistics for observables. For example, the kinetic

friction coefficient μ can be calculated by averaging the total instantaneous lateral friction force (F_{L}) and normal load (F_{N}) acting on the surface atoms under shear conditions. Each of these properties fluctuates significantly, and must be averaged over long simulations in order that the ratio $\mu = -F_{\mathrm{L}}/F_{\mathrm{N}}$ can be calculated reliably.

As with all molecular simulations, the choice of force field is an important factor. The DREIDING force field [36] and OPLS force field (in both all-atom and united-atom formulations) [37, 38] have been used in the work reviewed here. For model base oils, checks are made against experimental measurements of properties such as the density or viscosity, and deviations under ambient conditions are typically no more than 5% [31]. As will be shown in Sec. 4, the self-assembly of polar additives in bulk oil is described very accurately with standard force fields. The interactions between lubricants and surfaces are more complicated. For some minerals, such as mica, force fields specifically designed to describe interactions between inorganic and organic species are used, such as the INTERFACE-PCFF force field [39, 40, 41, 42]. Force fields are available for other commonly studied inorganic surfaces, such as iron oxide (α-Fe_2O_3) [24]. Of course, such force fields can only describe physisorption of surfactant-type molecules onto the substrate. Viable alternatives include reactive force fields such as ReaxFF [43], and *ab initio* MD methods, but the application to large-scale simulations is difficult. A proper account of chemisorption in MD simulations [44, 45], and the description of tribochemistry [46, 47] are ongoing problems.

3. Adsorption at the metal-oil interface

A good illustration of the 'classical' picture of lubrication is provided by the examples of stearic acid and oleic acid in squalane base oil [19]. The molecular structures of these molecules are shown in Fig. 2(a)–(c). Squalane is a convenient model of base oil, in that it has average molecular weight and viscometric properties. Fig. 2(d) shows an atomistic MD snapshot of stearic acid adsorbed

on parallel iron-oxide (α-Fe_2O_3) (100) surfaces at temperature $T = 298$ K and pressure $P = 10^8$ Pa. Clearly, the molecules form well-defined monolayers, although the surface coverage is somewhat less than the maximum values determined from adsorption-isotherm experiments (from dodecane) [48]. A recent computational and experimental study of stearic acid on iron oxide provides an explanation for this, on the basis of a random sequential adsorption model [49]. Note that the MD simulations are carried out with a classical force field, and so the additive molecules are physisorbed onto the surface.

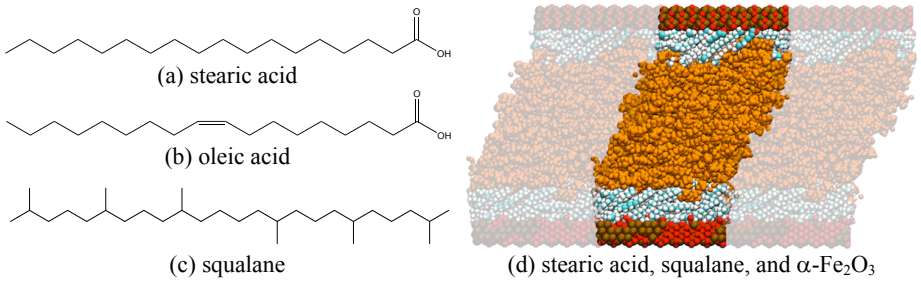

Figure 2: (a)–(c) Molecular structures of (a) stearic acid, (b) oleic acid, and (c) squalane. (d) Snapshot from a MD simulation of stearic acid adsorbed on iron-oxide (100) surfaces from squalane at $T = 298$ K and $P = 10^8$ Pa (adapted from Reference 19). The central simulation cell and two of its periodic replicas are shown. The stearic acid molecules are shown in blue and white, the squalane molecules are shown in gold, and the oxygen and iron atoms are shown in red and brown, respectively.

The frictional properties of these films were examined at $T = 298$ K and a load equivalent to $P = 10^8$ Pa by shearing the two parallel walls with relative velocity v_s, and measuring the ratio of the lateral and normal forces F_L and F_N, respectively. The extended Amontons-Coulomb law is $F_L = F_0 + \mu F_N$, where F_0 is a weak adhesive force known as the Derjaguin offset, and μ is the kinetic friction coefficient. Because the load is so high, $F_L \gg F_0$ [20], and so the friction coefficient is simply $\mu \simeq F_L/F_N$. It was found that μ increases first linearly with shear rate, and then logarithmically at high shear rates. The data can be fitted

extremely well with an Eyring-type model [50, 51, 19] given by

$$\mu = \mu_0 \ln \left[\left(\frac{\dot{\gamma}}{2\dot{\gamma}_0} \right) + \sqrt{1 + \left(\frac{\dot{\gamma}}{2\dot{\gamma}_0} \right)^2} \right] \tag{1}$$

where μ_0 and $\dot{\gamma}_0$ are fitting parameters. (An example is discussed in Sec. 5.) For a given surface coverage, it was observed that at all shear rates, the friction coefficient of stearic acid was higher than that of oleic acid. This was put down to more solid-like clustering of the saturated stearic acid molecules, arising from better packing. Films of unsaturated oleic acid molecules were more disordered, and therefore provided a less rigid layer on the iron-oxide surface. The difference between stearic acid and oleic acid decreased with increasing surface coverage, as the films resemble each other more when the molecules are packed together densely. These results on the effects of saturation are not immediately applicable to lubricants, however, because the surface coverage is not controlled in an engine. Instead, it is the bulk concentration of additive that is controlled, and stearic acid has a stronger adsorption than oleic acid; fits to the Langmuir isotherm show that the maximum surface coverage is $\Gamma_{\max} = 6.2 \times 10^{-6}$ mol m^{-2} for stearic acid and $\Gamma_{\max} = 3.7 \times 10^{-6}$ mol m^{-2} for oleic acid [48]. This may go some way to explaining why, experimentally, stearic acid has better anti-friction properties than oleic acid [52].

In some cases, the detailed structures of the adsorbed films can be compared directly with experiment. For example, SFG spectroscopy and polarised neutron reflectometry experiments on hexadecylamine adsorbed from dodecane on to α-Fe_2O_3 at $T = 298$ K and $P = 10^5$ Pa show that the monolayer thickness is 1.6–2.0 nm, and the average molecular tilt angle is 48° with respect to the surface [53]. Atomistic MD simulations show that the monolayer is 1.5–2.0 nm thick, and the average molecular tilt angle is 40° [20].

Finally, it should be noted that in simulations, the surfaces are often modeled as being perfectly smooth and parallel, but not always [54, 55]. In experimental investigations of adsorbed-film structures, the surfaces should be as flat as possible, and a small degree of roughness should be taken into account. One inter-

esting problem is how the adsorption of molecules depends on surface curvature, with all other parameters being held equal (specifically, bulk concentration and adsorption energy). This situation was studied using a coarse-grained model of surfactant molecules in an implicit solvent, adsorbing on to structureless spherical surfaces with a fixed radius of curvature R [56]. It was found that, for a given bulk concentration of surfactant, the adsorption decreases with increasing particle radius. As an example, for a bulk concentration corresponding to about 1×10^{-3} mol L^{-1}, the adsorption on a particle with $R = 0.8$ nm was about 80% higher than that on a particle with $R = 4.0$ nm ($\Gamma = 4.5 \times 10^{-6}$ mol m^{-2} versus $\Gamma = 2.5 \times 10^{-6}$ mol m^{-2}). An analysis of the various contributions to the adsorption free energy shows that the positive entropic component, arising from packing of the surfactant tail groups, is less for the small particle than for the large particle. (Note that the energetic component, representing binding of the head group to the surface, is the same in both cases.) For the small particle, the tail groups splay out radially from the surface, whereas for the large particle – and planar surfaces – the tail groups are (on average) parallel with one another. This is shown schematically in Fig. 1(a) and (c). Hence, the steric interactions are greater on flat surfaces than on highly curved surfaces. Not only does this reduce the adsorption on flat surfaces, but it also introduces a larger barrier in the free-energy profile along the 'reaction coordinate' defined by the distance between the polar head group and the surface. This barrier affects the adsorption and desorption kinetics.

4. Self-assembly in non-aqueous solution

OFMs are often surfactant-like molecules with polar head groups and non-polar tail groups. A classic example of an OFM is glycerol monooleate (GMO), the molecular structure of which is shown in Fig. 3(a). Remarkably, GMO and related molecules form reverse micelles in bulk solution [57, 58, 59, 60, 30, 31, 61]. A snapshot from an atomistic MD simulation of 5 wt% GMO in n-heptane is shown in Fig. 3(b). The choice of n-heptane as a base oil is important, because it

is readily available in deuterated form, which can be used in small-angle neutron scattering (SANS) experiments to improve contrast between solute and solvent. Such experiments have been done to determine the radius of gyration of the GMO reverse micelles. Fig. 3(c) shows the form factor $P(q)$ of GMO reverse micelles in n-heptane as determined from SANS and MD simulations [30]. q is the scattering wave vector. Fitting the data to a Gaussian model

$$\frac{P(q)}{P(0)} = \exp\left(-q^2 R_{\mathrm{g}}^2/3\right) \tag{2}$$

gives $R_{\mathrm{g}} = (1.663 \pm 0.007)$ nm (SANS) and $R_{\mathrm{g}} = (1.552 \pm 0.004)$ nm (MD), which shows remarkable consistency. In n-heptane, the aggregation number in the reverse micelle is about 30 molecules, while in toluene, the number is about 20 molecules. Nonetheless, the radius of gyration is roughly the same in both solvents, which reflects the different levels of solvation of the non-polar tail groups by the solvents [30].

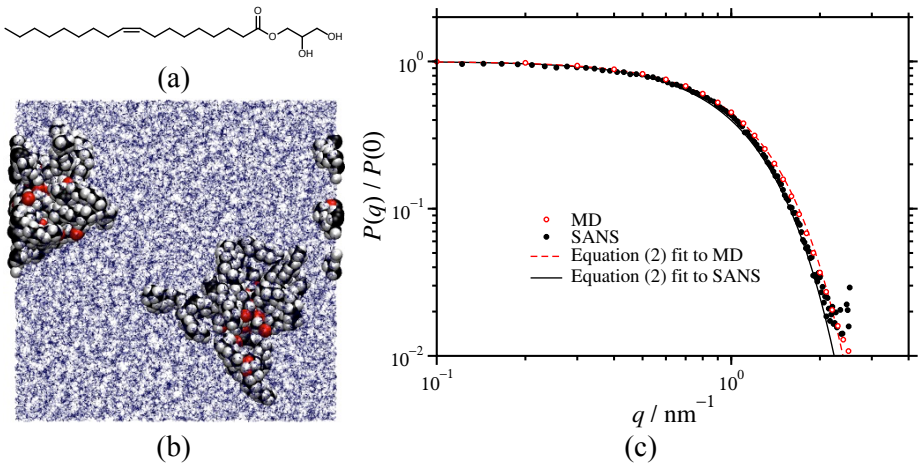

Figure 3: (a) Molecular structure of glycerol monooleate (GMO). (b) MD snapshot of GMO in n-heptane at $P = 10^5$ Pa and $T = 298$ K (adapted from Reference 30). The solvent is shown in a stick representation. The atoms in GMO are shown in red (oxygen), black (carbon), and white (hydrogen). (c) Form factor of reverse micelles in GMO from SANS (filled black points) and MD simulations (open red points) (data taken from Reference [30]). The solid black and dashed red lines are fits of Eq. (2) to the SANS and MD data, respectively, in the range $q \leq 1$ nm^{-1}.

Another aspect of self-assembly in bulk-solution conditions involves functionalised polymeric additives, which can be used as viscosity modifiers, friction modifiers, anti-wear agents, etc. The central question is whether the distribution of functional groups along a polymer backbone can affect the size of the polymer, as measured by either the radius of gyration R_{g}, or the end-to-end distance R_{ee} [62]. Fig. 4 shows simulation snapshots of one unfunctionalised polyethylene-polypropylene copolymer, and five functionalised polymers with the same composition (approximately 10 kDa, 240 monomer units and 8 functional groups per molecule), dissolved in n-heptane at $T = 298$ K and $P = 10^5$ Pa. The chemical details of the functional groups are proprietary, but the essential point is that they are solvophobic and are expected to associate reversibly in the solution. The molecules are very flexible, and the sizes undergo substantial thermal fluctuations, but the average values depend sensitively on the functional-group distribution, as shown in Fig. 4. Moreover, the shear viscosity η of the polymer solution (as measured in the MD simulations) is strongly correlated with the polymer size. η was measured in equilibrium MD simulations using the Einstein relation

$$\eta = \frac{V}{20k_{\mathrm{B}}T} \lim_{t\to\infty} \frac{\mathrm{d}}{\mathrm{d}t} \left\langle \sum_{\alpha\beta} \left[G_{\alpha\beta}(t) - G_{\alpha\beta}(0)\right]^2 \right\rangle \tag{3}$$

where V is the system volume, $G_{\alpha\beta} = \int_0^t P_{\alpha\beta}(t')\mathrm{d}t'$, $P_{\alpha\beta}$ is an element of the symmetrised traceless portion of the stress tensor, and $\alpha, \beta = x, y, z$ [63, 64, 65]. The results show that η increases with increasing R_{g}.

These two examples show that lubricant additives in bulk solution can undergo self-assembly. Hence, self-assembly may compete with adsorption and friction reduction, and this is discussed in Sec. 5.

5. Competition between adsorption and self-assembly

Fig. 5(a)–(c) shows simulation snapshots of 10 wt% GMO in squalane confined between α-Fe_2O_3 (100) surfaces at $T = 353$ K and loads of (a) $P = 10^5$ Pa, (b) $P = 10^8$ Pa, and (c) $P = 10^9$ Pa. The surfaces were in relative motion with $v_{\mathrm{s}} = 10$ m s^{-1} and shear rate $\dot{\gamma} \sim 10^9$ s^{-1}. At low pressure, the GMO is mostly

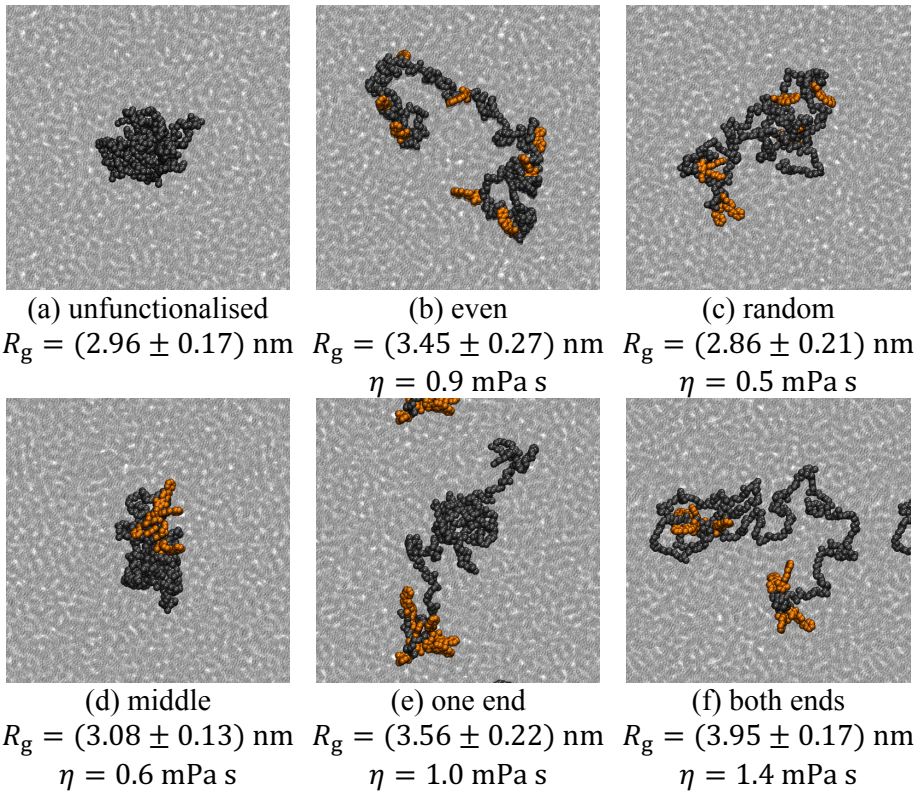

Figure 4: Snapshots from MD simulations of polymers in n-heptane at $T = 298$ K and $P = 10^5$ Pa (new snapshots adapted from Reference 62): (a) unfunctionalised polyethylene-polypropylene copolymer backbone; (b) even distribution of functional groups; (c) random distribution of functional groups; (d) all of the functional groups in the middle; (e) all of the functional groups at one end; (f) functional groups split evenly between both ends. The solvent is shown in a transparent representation, the polymer backbone atoms are shown in dark gray, and the functional group atoms are shown in orange. Also shown is the radius of gyration R_g (data taken from Reference 62) and the shear viscosity η (new data).

aggregated in to a reverse micelles, even under shear conditions. As the pressure is increased, the degree of aggregation decreases, and the adsorption on the surfaces increases. This shows that, under engine conditions, additive molecules may show a competition between adsorption and self-assembly.

The impact on friction can be assessed by measuring the friction coefficient μ in MD simulations. Fig. 5(d) shows μ as a function of $\dot{\gamma}$ for the same GMO system, from MD simulations and a fit according to Eq. (1). The quality of the fit is excellent, and in this case $\mu_0 = 0.110 \pm 0.009$ and $\dot{\gamma}_0 = (2.3 \pm 0.3) \times 10^8$ s^{-1}. $\dot{\gamma}_0$ gives a rough indication of where μ switches over from a linear dependence on low shear rates ($\mu \approx \mu_0 \dot{\gamma}/2\dot{\gamma}_0$), and a logarithmic dependence on high shear rates [$\mu \approx \mu_0 \ln(\dot{\gamma}/\dot{\gamma}_0)$].

There are at least two interesting effects concerning the impact of self-assembly on friction.

First, under engine conditions, the additive molecules can undergo a mixture of thermal and chemical degradation, e.g., hydrolysis. To assess the impact of such effects, the structural and tribological properties of GMO and its hydrolysis products were surveyed extensively [61]. The hydrolysis products included oleic acid and glycerol, and the solution of GMO and/or its hydrolysis products was confined between mica surfaces at $P = 10^5$ Pa and $T = 298$ K. Keeping the additive content fixed at 10 wt% in n-heptane, it was observed that hydrolysis leads to an increase in μ, and that after complete hydrolysis of GMO, the friction coefficient had increased by 50%. This is correlated with rather subtle structural changes. GMO itself adsorbs on to mica surfaces from heptane in the form of surface (hemi-)micelles, while the hydrolysis products adsorb more weakly. Hence, hydrolysis leads to a decrease of the amount of additive on the surfaces, and a concomitant increase in friction.

The second effect is the interaction between lubricant additives. Lubricants are extremely complex fluids, and to date, there has not been a systematic survey of the cooperative and/or competing interactions between different additives. In recent work, the interaction between OFMs and dispersants (used to keep soot in solution) has been studied in MD simulations, and some significant effects on

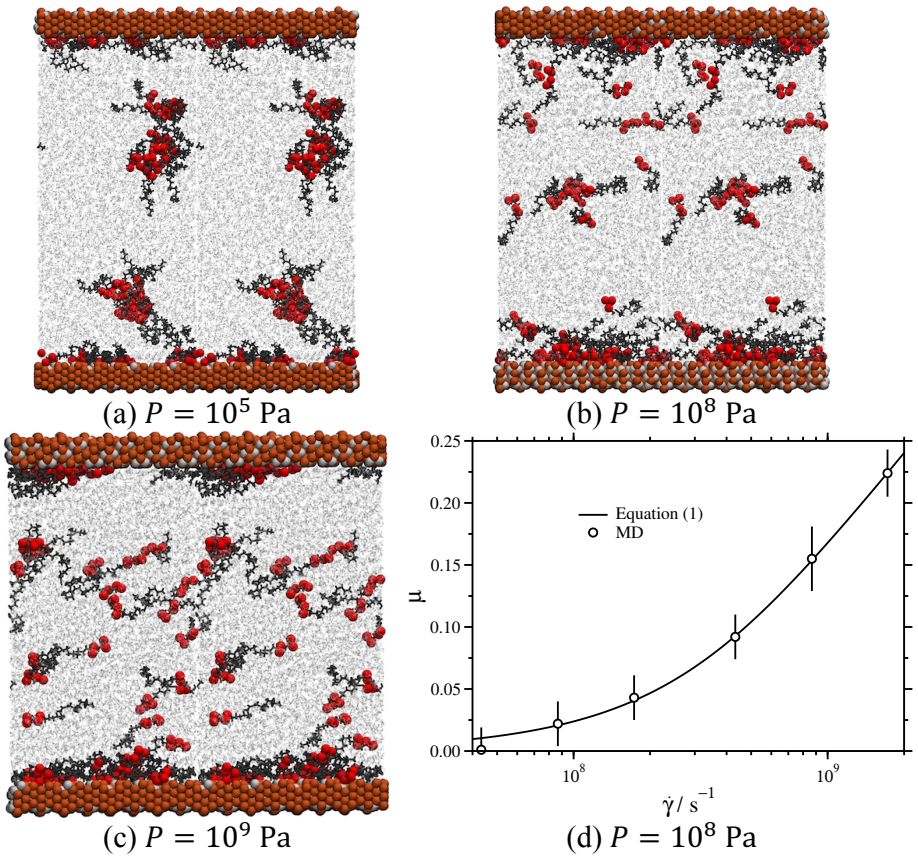

Figure 5: (a)–(c) Snapshots from MD simulations of 10 wt% GMO in squalane confined between α-Fe_2O_3 (100) surfaces at $T = 353$ K and (a) $P = 10^5$ Pa, (b) $P = 10^8$ Pa, and (c) $P = 10^9$ Pa. The solvent is shown in a transparent representation, the oxygen atoms of GMO are shown in red (to highlight association of the polar groups), and the oleate tails are shown as black sticks. Two periodic replicas are shown in each case. The surfaces are identical in all simulations, but thermal fluctuations and the periodic boundary conditions mean that atoms may appear on one side or the other of the primary simulation cell. (d) Friction coefficient μ as a function of shear rate $\dot{\gamma}$ in confined liquid layers of 10 wt% GMO in squalane at $P = 10^8$ Pa [66].

friction have been uncovered. The results of this work (by two of the authors, GT and PJC) are currently being prepared for publication [66].

6. Conclusions

Molecular simulations of additive adsorption, self-assembly, and friction in oils can be used to demonstrate some very complex behaviour which may have a direct effect on the performance of lubricants. In the classical picture, additive molecules are surfactant-like species which form monolayers on the surfaces of moving parts of an engine. This gives a reduction in the ordering of the oil at the solid-oil interface, which is correlated with a reduction in friction. An example of such classical lubrication is by carboxylic acids adsorbed on iron-oxide surfaces [19]; indeed, this was first considered in the 1920s [2, 3, 4]. Recent work shows that some surfactant-like additives self-assemble in bulk solution, leading to the formation of structures such as reverse micelles. An example is glycerol monooleate, a very widely used organic friction modifier, dissolved in simple hydrocarbon solvents [30]. In addition, functionalised polymers adopt very different conformations depending on how the functional groups are distributed along the polymer backbone [62]. These types of structures can persist under confinement between moving surfaces (such as in engines) and compete with monolayer adsorption. The balance of self-assembly and adsorption has been shown to have an impact on the friction coefficient; this has been illustrated in the case of glycerol monooleate in various solvents, confined between inorganic surfaces [31, 61]. Therefore, to establish structure-property relationships in lubricants, it is essential to understand first how molecular structure dictates the fundamental processes of adsorption and self-assembly. Lubricants are extremely complex fluids, and having discovered how several different types of additives behave in isolation, it is now important to learn how interactions between different additives can lead to either competitive or cooperative effects. There is a lot of work left to do, both experimentally and in molecular simulations.

Acknowledgements

The authors thank Beatrice Cattoz (Infineum), Peter Dowding (Infineum), Andrew Schwarz (Infineum), and Chris Warrens (BP Castrol) for collaboration. Funding from BP Castrol and Infineum to support G. T. and R. F. G. A., respectively, is gratefully acknowledged.

References

[1] F. Pearce, How 16 ships create as much pollution as all the cars in the world, *Daily Mail*, 21 November 2009, Available at: https://www.dailymail.co.uk/sciencetech/article-1229857/How-16-ships-create-pollution-cars-world.html [Accessed 29 October 2018].

[2] W. Hardy, I. Bircumshaw, Boundary lubrication. plane surfaces and the limitations of amontons' law, Proc. R. Soc. Lond. A 108 (1925) 1–27.

[3] F. P. Bowden, J. N. Gregory, D. Tabor, Lubrication of metal surfaces by fatty acids, Nature 156 (1945) 97–101.

[4] F. P. Bowden, D. Tabor, The Friction and Lubrication of Solids, revised Edition, Oxford University Press, 2001.

[5] J. P. Ewen, C. Gattinoni, F. M. Thakkar, N. Morgan, H. A. Spikes, D. Dini, A comparison of classical force-fields for molecular dynamics simulations of lubricants, Materials 9 (2016) 651–667.

[6] J. P. Ewen, D. M. Heyes, D. Dini, Advances in nonequilibrium molecular dynamics simulations of lubricants and additives, Friction 6 (2018) 349–386.

[7] S. A. Gupta, H. D. Cochran, P. T. Cummings, Shear behavior of squalane and tetracosane under extreme confinement. iii. effect of confinement on viscosity, J. Chem. Phys. 107 (1997) 10335–10343.

[8] M. L. Greenfield, H. Ohtani, Molecular dynamics simulation study of model friction modifier additives confined between two surfaces, Tribol. Lett. 7 (1999) 137–145.

[9] S. Bair, C. McCabe, P. T. Cummings, Comparison of nonequilibrium molecular dynamics with experimental measurements in the nonlinear shear-thinning regime, Phys. Rev. Lett. 88 (2002) 058302.

[10] S. T. Cui, C. McCabe, P. T. Cummings, H. D. Cochran, Molecular dynamics study of the nano-rheology of n-dodecane confined between planar surfaces, J. Chem. Phys. 118 (2003) 8941–8944.

[11] I. M. Sivebaek, V. N. Samoilov, B. N. J. Persson, Velocity dependence of friction of confined hydrocarbons, Langmuir 26 (2010) 8721–8728.

[12] M. R. Farrow, A. Chremos, P. J. Camp, S. G. Harris, R. F. Watts, Molecular simulations of friction modification in nanoscale fluid layers, Tribol. Lett. 42 (2011) 325–337.

[13] I. M. Sivebaek, V. N. Samoilov, B. N. J. Persson, Effective viscosity of confined hydrocarbons, Phys. Rev. Lett. 108 (2012) 036102.

[14] X. Zheng, H. Zhu, A. K. Tieu, K. Chen, Molecular dynamics simulation of confined n-alkanes: Ordered structure and crystalline bridges, Int. J. Surface Science and Engineering 8 (2014) 201–212.

[15] J. L. Rivera, G. K. Jennings, C. McCabe, Examining the frictional forces between mixed hydrophobic-hydrophilic alkylsilane monolayers, J. Chem. Phys. 136 (2012) 244701.

[16] S. M. Lundgren, M. Ruths, K. Danerlöv, K. Persson, Effects of unsaturation on film structure and friction of fatty acids in a model base oil, J. Colloid Interface Sci. 326 (2008) 530–536.

[17] M. Ruths, S. Lundgren, K. Danerlöv, K. Persson, Friction of fatty acids in nanometer-sized contacts of different adhesive strength, Langmuir 24 (2008) 1509–1516.

[18] S. Eder, A. Vernes, G. Betz, On the derjaguin offset in boundary-lubricated nanotribological systems, Langmuir 29 (2013) 13760–13772.

[19] M. Doig, C. P. Warrens, P. J. Camp, Structure and friction of stearic acid and oleic acid films adsorbed on iron-oxide surfaces in squalane, Langmuir 30 (2014) 186–195.

[20] M. Doig, P. J. Camp, The structures of hexadecylamine films adsorbed on iron-oxide surfaces in dodecane and hexadecane, Phys. Chem. Chem. Phys. 17 (2015) 5248–5255.

[21] J. P. Ewen, C. Gattinoni, N. Morgan, H. A. Spikes, D. Dini, Nonequilibrium molecular dynamics simulations of organic friction modifiers adsorbed on iron oxide surfaces, Langmuir 32 (2016) 4450–4463.

[22] Y. Morita, S. Jinno, M. Murakami, N. Hatakeyama, A. Miyamoto, A computational chemistry approach for friction reduction of automotive engines, Int. J. Engine Res. 15 (2014) 399–405.

[23] J. E. Davidson, S. L. Hinchley, S. G. Harris, A. Parkin, S. Parsons, P. A. Tasker, Molecular dynamics simulations to aid the rational design of organic friction modifiers, J. Mol. Graphics Modell. 25 (2006) 495–506.

[24] H. Berro, N. Fillot, P. Vergne, Molecular dynamics simulation of surface energy and ZDDP effects on friction in nano-scale lubricated contacts, Tribol. Int. 43 (2010) 1811–1822.

[25] T. Onodera, Y. Morita, A. Suzuki, M. Koyama, H. Tsuboi, N. Hatakeyama, A. Endou, H. Takaba, M. Kubo, F. Dassenoy, C. Minfray, L. Joly-Pottuz, J.-M. Martin, A. Miyamoto, A computational chemistry study on friction of h-MoS_2. part i. mechanism of single sheet lubrication, J. Phys. Chem. B 113 (2009) 16526–16536.

[26] T. Onodera, Y. Morita, R. Nagumo, R. Miura, A. Suzuki, H. Tsuboi, N. Hatakeyama, A. Endou, H. Takaba, F. Dassenoy, C. Minfray, L. Joly-Pottuz, M. Kubo, J.-M. Martin, A. Miyamoto, A computational chemistry

study on friction of h-MoS_2 part ii. friction anisotropy, J. Phys. Chem. B 114 (2010) 15832–15838.

[27] F. F. Canova, H. Matsubara, M. Mizukami, K. Kurihara, A. L. Shluger, Shear dynamics of nanoconfined ionic liquids, Phys. Chem. Chem. Phys. 16 (2014) 8247–8256.

[28] A. C. F. Mendonça, A. A. H. Pádua, P. Malfreyt, Nonequilibrium molecular simulations of new ionic lubricants at metallic surfaces: Prediction of the friction, J. Chem. Theory Comput. 9 (2013) 1600–1610.

[29] J. P. Ewen, C. Gattinoni, F. M. Thakkar, N. Morgan, H. A. Spikes, D. Dini, Nonequilibrium molecular dynamics investigation of the reduction in friction and wear by carbon nanoparticles between iron surfaces, Tribol. Lett. 63 (2016) 1–15.

[30] J. L. Bradley-Shaw, P. J. Camp, P. J. Dowding, K. Lewtas, Glycerol monooleate reverse micelles in nonpolar solvents: Computer simulations and small-angle neutron scattering, J. Phys. Chem. B 119 (2015) 4321–4331.

[31] J. L. Bradley-Shaw, P. J. Camp, P. J. Dowding, K. Lewtas, Molecular dynamics simulations of glycerol monooleate confined between mica surfaces, Langmuir 32 (2016) 7707–7718.

[32] M. P. Allen, D. J. Tildesley, Computer simulation of liquids, 2nd Edition, Oxford University Press, Oxford, 2016.

[33] D. Frenkel, B. Smit, Understanding Molecular Simulation: From Algorithms to Applications, 2nd Edition, Academic Press, San Diego, 2001.

[34] A. Martini, H.-Y. Hsu, N. A. Patankar, S. Lichter, Slip at high shear rates, Phys. Rev. Lett. 100 (2008) 206001.

[35] H. Berro, N. Fillot, P. Vergne, T. Tokumasu, T. Ohara, G. Kikugawa, Energy dissipation in non-isothermal molecular dynamics simulations of confined liquids under shear, J. Chem. Phys. 135 (2011) 134708.

[36] S. L. Mayo, B. D. Olafson, W. A. Goddard III, Dreiding: A generic force field for molecular simulations, J. Phys. Chem. 94 (1990) 8897–8909.

[37] W. L. Jorgensen, J. D. Madura, C. J. Swenson, Optimized intermolecular potential functions for liquid hydrocarbons, J. Am. Chem. Soc. 106 (1984) 6638–6646.

[38] W. L. Jorgensen, D. S. Maxwell, J. Tirado-Rives, Development and testing of the OPLS all-atom force field on conformational energetics and properties of organic liquids, J. Am. Chem. Soc. 118 (1996) 11225–11236.

[39] H. Heinz, H. J. Castelijns, U. W. Suter, Structure and phase transitions of alkyl chains on mica, J. Am. Chem. Soc. 125 (2003) 9500–9510.

[40] H. Heinz, U. W. Suter, Surface structure of organoclays, Angew. Chem. Int. Ed. 116 (2004) 2289–2293.

[41] H. Heinz, H. Koerner, K. L. Anderson, R. A. Vaia, B. L. Farmer, Force field for mica-type silicates and dynamics of octadecylammonium chains grafted to montmorillonite, Chem. Mater. 17 (2005) 5658–5669.

[42] H. Heinz, T.-J. Lin, R. K. Mishra, F. S. Emami, Thermodynamically consistent force fields for the assembly of inorganic, organic, and biological nanostructures: The interface force field, Langmuir 29 (2013) 1754–1765.

[43] K. Chenoweth, A. C. T. van Duin, W. A. Goddard III, Reaxff reactive force field for molecular dynamics simulations of hydrocarbon oxidation, J. Phys. Chem. A 112 (2008) 1040–1053.

[44] C.-L. Chia, C. Avendaño, F. R. Siperstein, S. Filip, Liquid adsorption of organic compounds on hematite α-Fe_2O_3 using reaxff, Langmuir 33 (2017) 11257–11263.

[45] C. Gattinoni, J. P. Ewen, D. Dini, Adsorption of surfactants on α-Fe_2O_3(0001): A density functional theory study, J. Phys. Chem. C 122 (2018) 20817–20826.

[46] N. J. Mosey, M. H. Müser, T. K. Woo, Molecular mechanisms for the functionality of lubricant additives, Science 307 (2005) 1612–1615.

[47] D.-C. Yue, T.-B. Ma, Y.-Z. Hu, J. Yeon, A. C. T. van Duin, H. Wang, J. Luo, Tribochemistry of phosphoric acid sheared between quartz surfaces: A reactive molecular dynamics study, J. Phys. Chem. C 117 (2013) 25604–25614.

[48] M. H. Wood, M. T. Casford, R. Seitz, A. Zarbakhsh, R. J. L. Welbourn, S. M. Clarke, Comparative adsorption of saturated and unsaturated fatty acids at the iron oxide/oil interface, Langmuir 32 (2016) 534–540.

[49] A. Jaishankar, A. Jusufi, J. L. Vreeland, S. Deighton, J. Pellettiere, A. M. Schilowitz, Adsorption of stearic acid at the iron oxide/oil interface – theory, experiments and modeling (unpublished).

[50] B. J. Briscoe, D. C. B. Evans, The shear properties of langmuir-blodgett layers, Proc. R. Soc. Lond. A 380 (1982) 389–407.

[51] S. Campen, J. Green, G. Lamb, D. Atkinson, H. Spikes, On the increase in boundary friction with sliding speed, Tribol. Lett. 48 (2012) 237–248.

[52] S. Hironaka, Friction properties of C_{18}-fatty acids, Sekiyu Gakkaishi 31 (1988) 216–220.

[53] M. H. Wood, R. J. L. Welbourn, T. Charlton, A. Zarbakhsh, M. T. Casford, S. M. Clarke, Hexadecylamine adsorption at the iron oxide-oil interface, Langmuir 29 (2013) 13735–13742.

[54] J. P. Ewen, S. E. Restrepo, N. Morgan, D. Dini, Nonequilibrium molecular dynamics simulations of stearic acid adsorbed on iron surfaces with nanoscale roughness, Tribol. Int. 107 (2017) 264–273.

[55] A. Porras-Vazquez, L. Martinie, P. Vergne, N. Fillot, Independence between friction and velocity distribution in fluids subjected to severe shearing and confinement, Phys. Chem. Chem. Phys. 20 (2018) 27280–27293.

[56] M. R. Farrow, P. J. Camp, P. J. Dowding, K. Lewtas, The effects of surface curvature on the adsorption of surfactants at the solid-liquid interface, Phys. Chem. Chem. Phys. 15 (2013) 11653–11660.

[57] L. K. Shrestha, O. Glatter, K. Aramaki, Structure of nonionic surfactant glycerol α-monomyristate micelles in organic solvents: A saxs study, J. Phys. Chem. B 113 (2009) 6290–6298.

[58] L. K. Shrestha, R. G. Shrestha, M. Abe, K. Ariga, Reverse micelle microstructural transformations induced by oil and water, Soft Matter 7 (2011) 10017–10024.

[59] R. G. Shrestha, L. K. Shrestha, K. Ariga, M. Abe, Reverse micelle microstructural transformations induced by surfactant molecular structure, concentration, and temperature, J. Nanosci. Nanotechno. 11 (2011) 7665–7675.

[60] L. K. Shrestha, R. G. Shrestha, K. Aramaki, J. P. Hill, K. Ariga, Nonionic reverse micelle formulation and their microstructure transformations in an aromatic solvent ethylbenzene, Colloids Surf. A 414 (2012) 140–150.

[61] J. L. Bradley-Shaw, P. J. Camp, P. J. Dowding, K. Lewtas, Self-assembly and friction of glycerol monooleate and its hydrolysis products in bulk and confined non-aqueous solvents, Phys. Chem. Chem. Phys. 20 (2018) 17648–17657.

[62] R. F. G. Apóstolo, P. J. Camp, B. N. Cattoz, P. J. Dowding, A. D. Schwarz, Effect of functional-group distribution on the structure of a polymer in non-aqueous solvent, Mol. Phys. 116 (2018) 2942–2953.

[63] P. J. Daivis, D. J. Evans, Comparison of constant pressure and constant volume nonequilibrium simulations of sheared model decane, J. Chem. Phys. 100 (1994) 541–547.

[64] M. Mondello, G. S. Grest, Viscosity calculations of n-alkanes by equilibrium molecular dynamics, J. Chem. Phys. 106 (1997) 9327–9336.

[65] T. Chen, B. Smit, A. T. Bell, Are pressure fluctuation-based equilibrium methods really worse than nonequilibrium methods for calculating viscosities?, J. Chem. Phys. 131 (2009) 246101.

[66] G. Tsagkaropoulou, C. P. Warrens, P. J. Camp, Interactions between friction modifiers and dispersants in lubricants: the case of glycerolmonooleate and polyisobutylsuccinimide-polyamine (unpublished).